Bu-Ali Sina University

The Effect of Pre-compaction on Properties of Mg/SiC Nanocomposites Compacted at High Strain Rates

G.H. Majzoobi[a,*], K. Rahmani[a], M. Kashfi[b]

[a]Mechanical Engineering Department, Bu-Ali Sina University, Hamedan, Iran.
[b]Mechanical Engineering Department, Ayatollah Boroujerdi University, Boroujerd, Iran.

Article info

Abstract

The effect of pre-compaction on mechanical properties of Mg/SiC nanocomposites prepared through dynamic compaction was investigated. The dynamic compactions were carried out at two different loading rates using Drop Hammer (DH) and Split Hopkinson Bar (SHB). The quasi-static pre-compaction was performed under two different pressures of 50 and 100MPa and at 450°C. The results show that the highest improvement in density, hardeness, and strength are obtained for the pre-compaction pressure of 50MPa. The reason is believed to be due to the discharge of the air packets trapped between the particles. For the pre-compaction pressure of 100MPa, however, density, strength, and hardness decrease. The reason is thought to be due to creation of cracks and faults in the specimens. The results indicate that there is an optimum for the pre-compaction pressure which varies depending on the type of matrix, reinforcing particles, and compaction loading rate.

1. Introduction

The common reinforcing particles used in magnesium composites are SiC, B4C, and Al_2O_3 [1]. Addition of ceramic nanoparticles to magnesium matrix can be accomplished by powder metallurgy. The compaction of powder can be performed quasi-statically or dynamically. Typical quasi-static methods for manufacturing reinforced nanocomposites are hot press [2], Hot Isostatic Press (HIP) [3], hot extrusion [4], and cold press, and sintering [5]. Dynamic compaction is performed using shockwaves [6, 7] and high velocity compaction [6]. The high velocity compaction processes, often employ an explosion or gas pressure to accelerate a projectile against the powder of the composite.

Rahmani et al. [8] fabricated Split Hopkinson Bar for dynamic compaction of Mg/SiC nanocomposites. Majzoobi et al. [9] fabricated Mg/SiC nanocomposites with different volume fractions of reinforcing particles

including 0, 1.5, 3, 5, and 10 vol% under dynamic loading using a Drop Hammer. Their report indicated an improvement in the strength and hardness of nanocomposite samples. Wang et al. [10] studied the improvement in density and mechanical properties of specimens fabricated by powder metallurgy using high velocity compaction. In contrast to the quasi-static processes, dynamic methods generate high local temperatures needed for initiation of metallurgic bonds at particle boundaries, while remaining the rest of the powder relatively cold. Therefore, dynamic compaction methods minimize the changes in microstructure such as agglomeration and grain growth due to the high temperature [11, 12]. In fact, dynamic compaction methods vanish the need for hot sintering that is generally required for metallurgic bonding at particle boundaries. In dynamic compaction, typically, the local heat generation causes the so-called cold sintering; however, this type of sintering may not be enough to reach the high-

est physical and mechanical properties. The literature review suggests that pre-compaction may be a complementary process to improve the compaction of powder under dynamic loading [13, 14].

In general, in dynamic powder compaction processes, there is no sufficient time to discharge the air trapped among particles. These packets of trapped air can prevent perfect bonding of the particles during the compaction process; hence, it reduces the final density of the fabricated sample. Therefore, samples are initially compressed under quasi-static condition to release the trapped air packets before dynamic compaction [15, 16]. Majzoobi et al. [17] showed that the quality of Al7075-B4C nanocomposites fabricated within the range of $1200s^{-1}$ to $1600s^{-1}$ was significantly improved for the pre-compacted samples. Literature review [15, 16] indicates that full powder consolidation may not be achieved if mechanical impedance of material is not big enough. Therefore, powder initial density must be increased to increase the sound speed in the powder, i.e. increasing the mechanical impedance. Additionally, pre-compaction reduces the deteriorating effects of the air trapped between the powder particles. The trapped air heats up due to the compaction shockwave and the resulting hot gas expands after removing the compaction pressure, thus it reduces the final sample density.

Unlike their previous study [17], Atrian et al. [18], showed the undesired effects of pre-compaction on the mechanical properties of Al6061/SiC nanocomposites fabricated by dynamic compaction; it was stated in that pre-compaction of powder followed by compaction process within the strain rates of $101s^{-1}$ to $103s^{-1}$ leads to lower density, hardness, and even strength of the compacts. Damage and embrittlement were observed in the samples compacted initially before dynamic compaction. Furthermore, some non-uniform behavior of pre-compaction (increase and then decrease or vice versa) was also seen in their investigations [18]. In addition, Hong et al. [19] studied the compaction of α-Al$_2$O$_3$ ceramic nanoparticles by magnetic pulse compaction; it was found that pre-compaction was effective on grain size, mechanical, and electrical properties of the fabricated specimens. In many investigations, the samples were subjected to quasi-static compaction to remove pores and trapped air from the powder before performing the main dynamic compaction and increases density and improves mechanical properties of the compacted specimens [19, 20]. However, the study of pre-compaction has been part of some investigations [17-20] in recent years.

In the present study, the Mg/SiC nanocomposites powder were initially compacted under uniaxial quasi-static loading at the pressures of 50 and 100MPa using an Instron testing device. The pre-compacted Mg/SiC nanocomposites were then compacted through hot dynamic loading using Split Hopkinson Bar and Drop Hammer. Eventually, the effects of quasi-static pre-compaction and volume percentage of reinforcement on mechanical properties and microstructure of samples were investigated.

2. Equipment and Experiments

2.1. Materials

Mg/SiC nanocomposites were prepared using Magnesium powder with purity of 99.5% and particle size of $100\mu m$ as the matrix and SiC nanoparticles with purity of 99% and average size of 75nm as the reinforcing particles. The specimens of nanocomposite containing 0, 1.5, 3, 5, and 10 vol% SiC nanoparticles were fabricated. The details of the mixing procedure and the methods of preventing oxidation and agglomeration can be found in [21]. Figs. 1a and 1b illustrate the SEM micrographs of surface morphology of Mg particles before and after mixing with SiC nanoparticles. As the figure indicates, SiC nanoparticles have fully covered the surface of Mg particles. Moreover, Transmission Electron Microscopy (TEM) and Field Emission Scanning Electron Microscopy (FESEM) images of SiC nanoparticles are shown in Fig. 1(c, d). The XRD patterns of the powder after 1h of milling are demonstrated in Fig. 2. The figure indicates that no new phase was generated in the composite after mixing.

2.2. High Rate Hot Compaction

Nanocomposite samples were produced under two different strain rates of $1000s^{-1}$ and $1600s^{-1}$ using Drop Hammer (DH) and Split Hopkinson Bar (SHB), respectively [17, 22]. The energy for the compactions at strain rate of $1000s^{-1}$ was supplied by a Dropping Hammer of 60kg and dropping height of 3.5 meters. The details of the Drop Hammer can be found in reference [9]. The energy for the compactions at strain rate of $1600s^{-1}$ was supplied by a Split Hopkinson Bar the details of which can be found in reference [21]. Three pre-compaction pressures of $P_1 = 0$MPa (no pre-compaction), $P_2 = 50$MPa, and $P_3 = 100$MPa were used to study the effect of pre-compaction. Pre-compaction of powders was carried out using an Instron universal testing machine. Cylindrical samples with length of 10^{-12}mm and diameter of 15mm were produced during the pre-compaction process. The compactions were carried out at 450°C which is almost equal to the sintering temperature of magnesium [23]. This temperature was generated using a ceramic heating element with the power of 1200 Watts. The density of the pre-compacted specimens was around 55% of the theoretical density. MoS$_2$ lubricant was used to minimize the friction between powder and mold and reaching the highest and homogenous distribution of density in specimens. The lubrication also enhances the qual-

ity of the samples and diminishes the roughness of the specimen's surfaces. The compaction conditions are summarized in Table 1.

3. Characterizing Examinations

In order to investigate the effects of pre-compaction and volume fraction of nanoparticles on the physical and mechanical properties of magnesium-based nanocomposites, the following examinations were carried out:

a) Microstructural characteristics including morphology powder, particle structure, grain size, uniformity of the nanoparticles distribution, porosities and bonding behavior were examined using Optical Microscopy (OPM) and Field Emission Scanning Electron Microscopy (FE-SEM). The FESEM was performed at Iran Poly-

mer and Petrochemical Institute. For this purpose, the specimens were polished up to $0.05\mu m$ and were etched for 7 seconds using 70ml ethanol solution, 4.2g picric acid, 10ml acetic acid and 10ml water according to the ASTM E 407-99 standards [24].

b) X-ray diffraction (XRD) was used to investigate the changes in the crystalline structure and also, to observe the crystalline patterns of samples. XRD analysis was performed on polished specimens utilizing a Philips X'PERT PW3040 diffractometer (40kV/30mA) with Cu Ka radiation ($k = 0.154059$nm) and scanning speed of $2°$/min. The XRD examinations were performed at Bu-Ali Sina University.

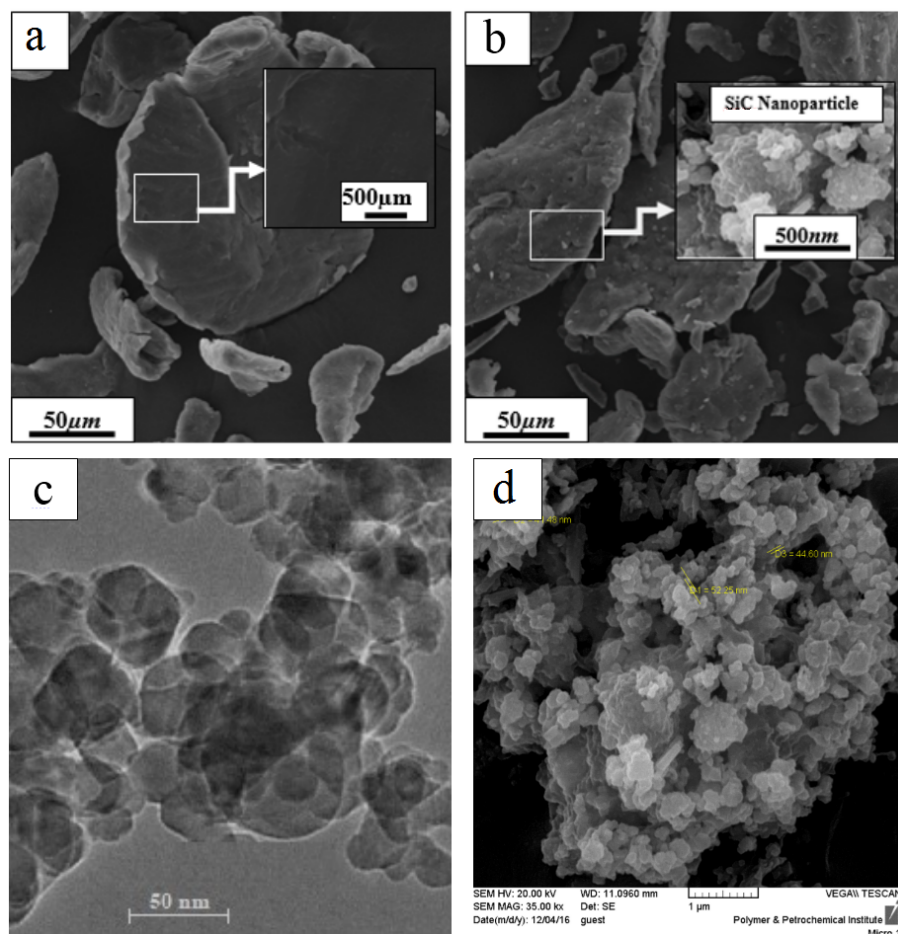c) Archimedes method [21] was used to measure the relative density of the compacted samples.

Fig. 1. Images of a) Mg, b) Mg-5 vol.% SiC after 1 h of ball milling, c) Transmission electron microscopy (TEM), and d) scanning electron microscopy (FESEM) of SiC nanoparticles.

Table 1
Compaction conditions.

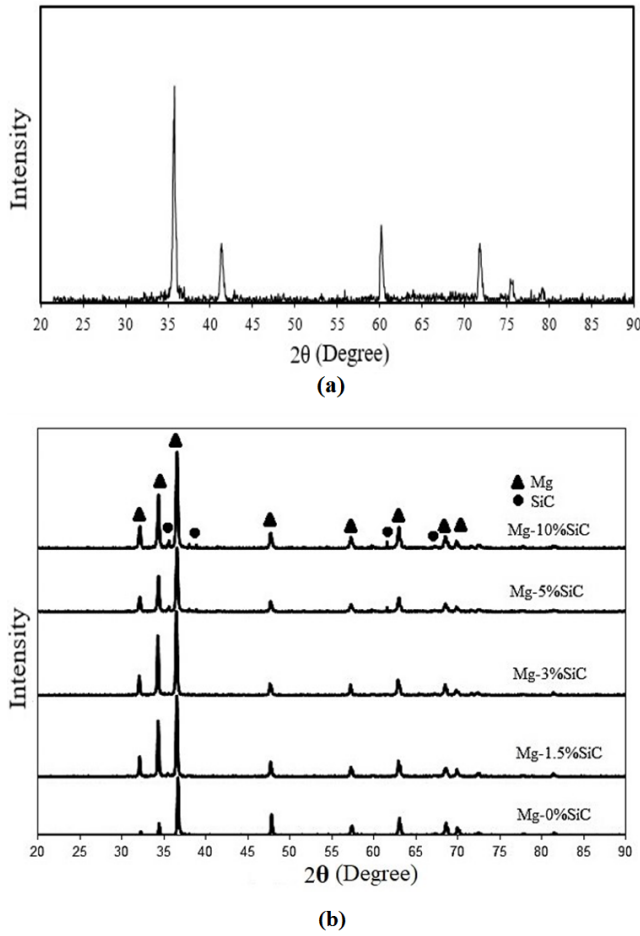| Powder type	Temperature (°C)	SiC content (vol.%)	Pre-compaction stress (MPa)
Mg/SiC	450	0, 1.5, 3, 5, 10	0, 50, 100

(a)

(b)

Fig. 2. a) XRD pattern of SiC nanoparticles, b) XRD patterns of powder after 1h of milling: Mg; Mg-1.5 vol.% SiC; Mg-3 vol.% SiC; Mg-5 vol.% SiC; Mg-10 vol.% SiC.

d) The micro-hardness tests were conducted based on ASTM E384-99 standards [25] and hardness was measured using a micro hardness tester manufactured by Buehler Company Ltd. The surface of samples was polished first and then Vickers hardness was measured at six points (three on the top and three on the bottom surface) by applying a load of 100gf in 15s. The average of readings was considered as the hardness of the sample.

e) Conventional compression tests were conducted based on ASTM E9 89a standards [26] on the compacted samples at strain rate of $0.008s^{-1}$ using an Instron testing machine.

4. Results and Discussion

4.1. Microstructural Examination

The effects of pre-compaction on surface quality and microstructural evolution of pure Mg samples are shown in Figs. 3 and 4, respectively. It is obvious in the figures that the compaction under the pressure of 50MPa yielded (i) the best surface quality and (ii) less porosity in the specimens was produced using dynamic compaction. This is, as stated before [13, 27] due to the fact that during pre-compaction stage, there is sufficient time for discharging the air trapped between powder particles.

SEM images of pre-compacted samples fabricated using DH and SHB, are illustrated in Figs. 5 and 6, respectively. As the figures suggest, the porosities and cracks of samples with pre-compaction ($P = 50$MPa) (Figs. 5b and 6b) decreased compared to those in the samples without pre-compaction (Figs. 5a and 6a). Moreover, stronger bonds between magnesium and reinforcing particles along the grain boundaries are observed for the samples pre-compacted at the pressure of 50MPa. This is while for the pre-compaction pressure of 100MPa, large number of cracks, pores, and fractures can be observed at grain boundaries (Figs. 5c and 6c). Furthermore, the increase of pre-compaction pressure from 50 to 100MPa may give rise to reduction of sample resistance against reflected stretching waves which cause fractures similar to those observed in the SEM images [6].
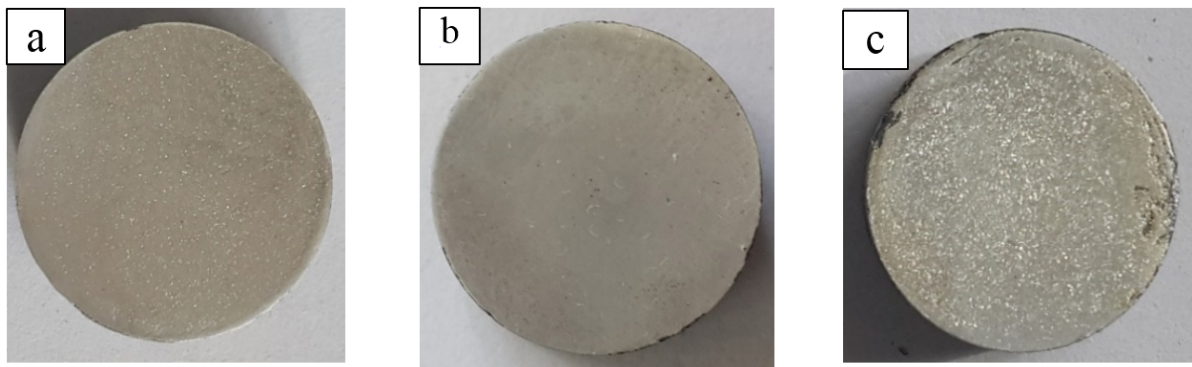

Fig. 3. Pre-compacting effect on the quality of pure Mg samples a) Without pre-compaction, b) With pre-compaction at 50MPa, c) With pre-compaction at 100MPa.
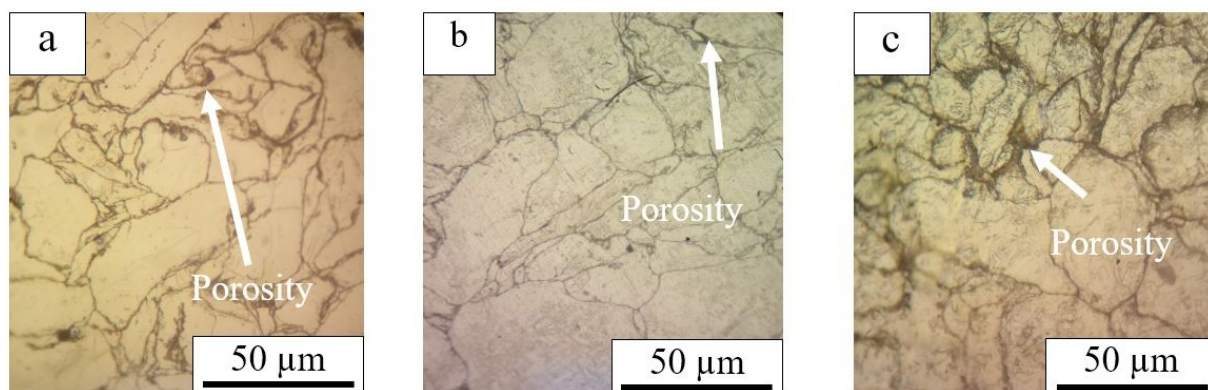
Fig. 4. The microstructure of the pure Mg samples compacted, a) Without pre-compaction, b) With pre-compaction at 50MPa, c) With pre-compaction at 100MPa.
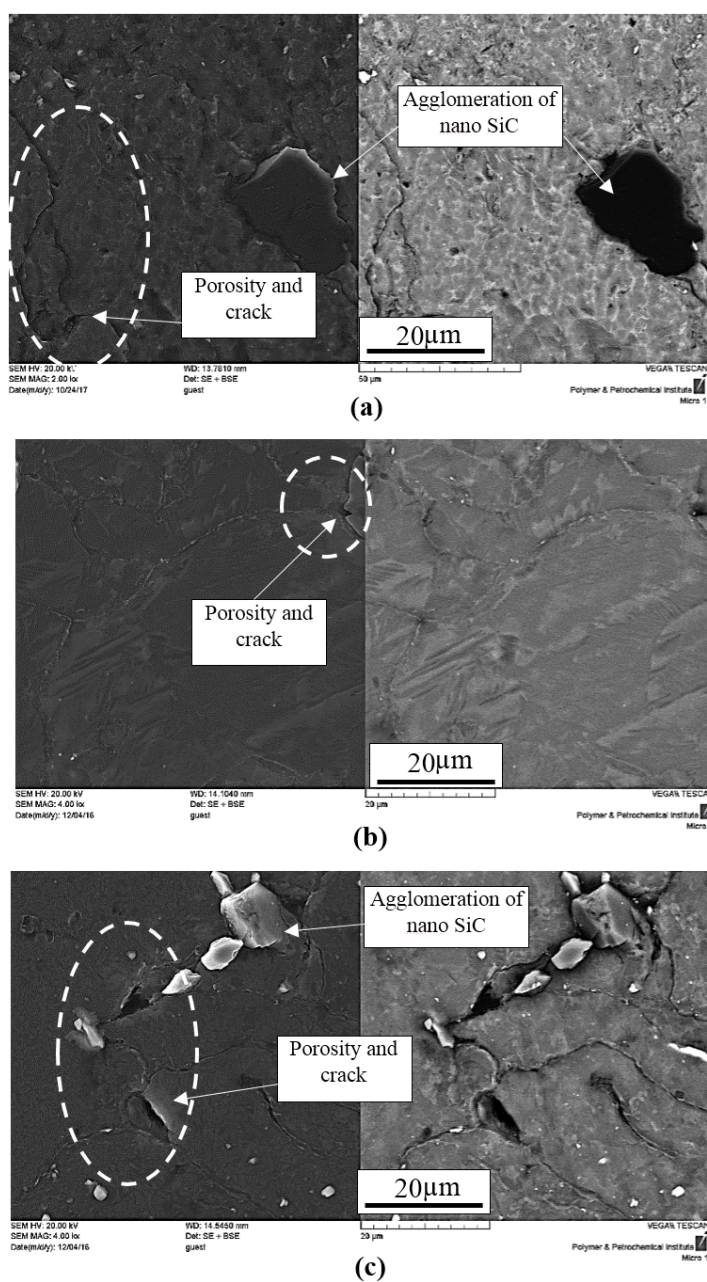

Fig. 5. Microstructure of Mg-5vol.% SiC nanocomposite samples compacted by DH, a) Without pre-compaction, b) With pre-compaction at 50MPa, c) With pre-compaction at 100MPa.
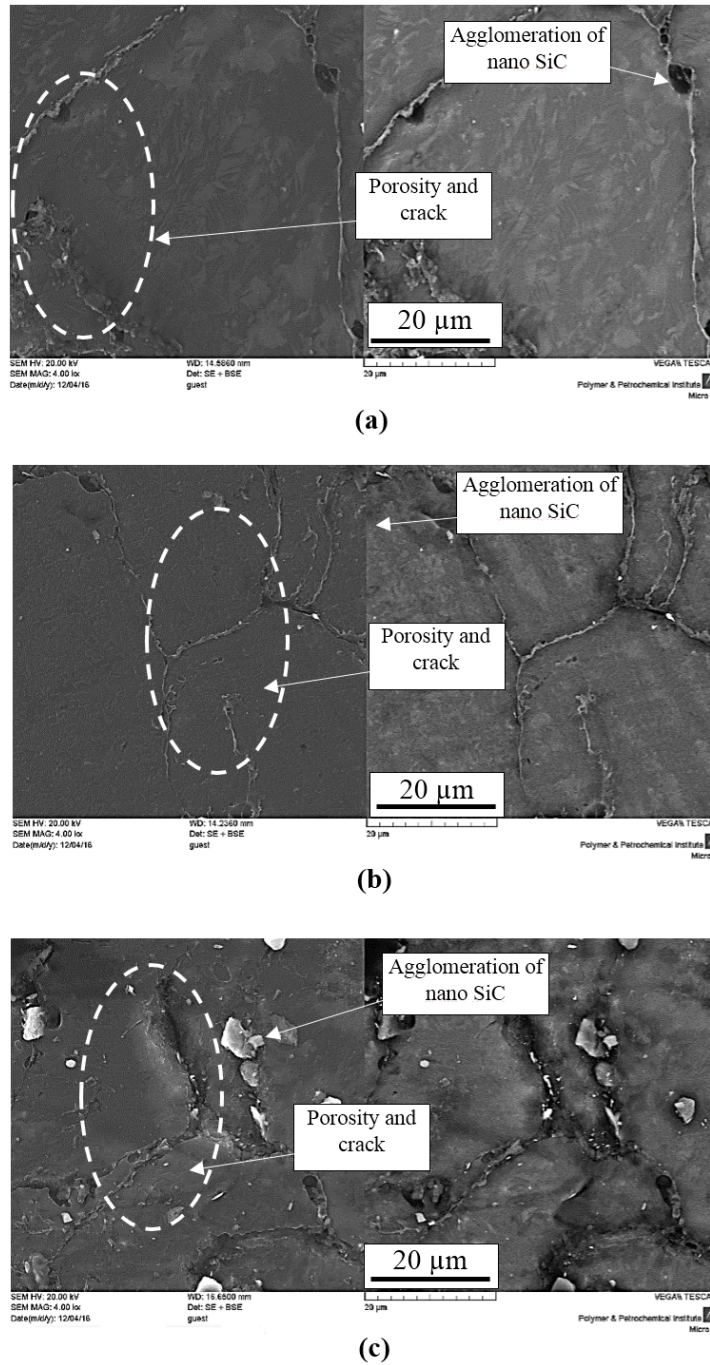
(a)

(b)

(c)

Fig. 6. Microstructure of Mg-5vol.%SiC nanocomposite compacted by SHB a) Without pre-compaction, b) With pre-compaction at 50MPa, c) With pre-compaction at 100MPa.

4.2. Relative Density

Variation of relative density for different pre-compaction pressures and different volume fractions of nanoparticles in sample fabricated using DH and SHB are shown in Fig. 7. As it is observed, relative density diminishes with the increase of nanoparticles volume fraction. Pre-compaction increases the initial relative density of 55% of theoretical density for nanocomposite powder samples to 70 to 80% of the theoretical value.

As Fig. 7 implies, the samples pre-compacted at the pressure of 50MPa are compacted more perfectly, so their relative density may reach 99.9%. However, for the pre-compaction pressure of 100MPa relative density reduces compared with that for the pressure of 50MPa. This agrees well with microstructural examinations discussed earlier in section 4.1. Furthermore, Relative density of the samples fabricated at different pre-compaction pressure and compacted dynamically under different rates of loading is shown in Fig. 8.
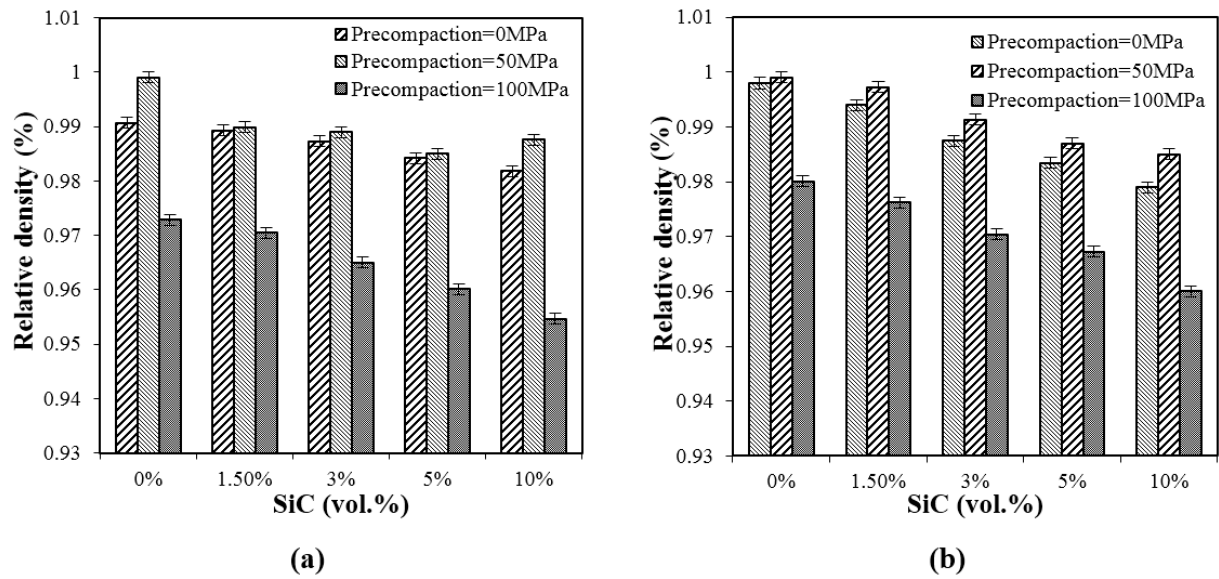
Fig. 7. Pre-compaction effect on relative density of nanocomposites fabricated by (a) DH (b) SHB.
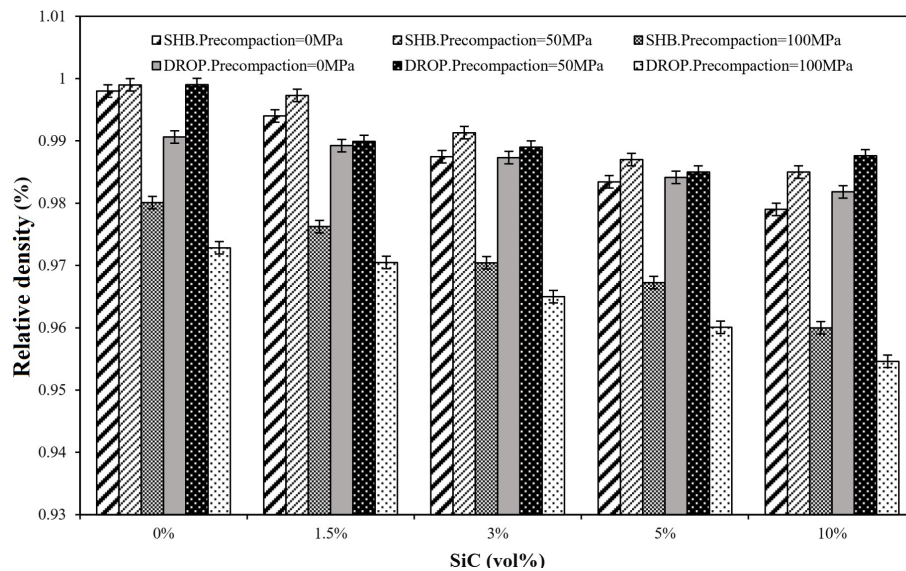

Fig. 8. Relative density of the samples fabricated at different pre-compaction pressure and compacted dynamically under different rates of loading.

4.3. Mechanical Properties

4.3.1. Microhardness

The effect of quasi-static pre-compaction on microhardness of Mg/SiC nanocomposites for various volume percentages of SiC, fabricated using DH and SHB are presented in Fig. 9. As the figure indicates, increase in the SiC nanoparticle content results in increase in microhardness. The improvement in microhardness is due to the increase in nanoparticle content and uniform distribution of reinforcing nanoparticle phase [28]. The presence of SiC nanoparticles with higher hardness can limit the local deformation during compaction (hardening effect of SiC particles). The uniform distribution of reinforcing phase can also im-

prove sample hardness due to hardness of nanoparticles present in the structure [21, 28]. In addition, similar trend for variation of hardness versus pre-compaction pressure as was observed for relative density and microstructural changes can be seen in Fig. 9. The figure shows that higher hardness is achieved in the samples with pre-compaction. Similar results were reported by Yi et al. [20]. Fig. 9 also shows that for the pre-compaction of 50MPa, the microhardness of Mg-10vol.%SiC samples fabricated using SHB and DH, increased by 2.6% and 6.7%, respectively. This is while, for the pre-compaction of 100MPa, microhardness of Mg-10vol.%SiC samples fabricated using SHB and DH decreased by 10% and 13%, respectively compared with the same samples without pre-compaction.

4.3.2. Compressive Strength

The stress-strain curves for Mg–10vol.%SiC nanocomposites fabricated using SHB at different pre-compaction pressures are presented in Fig. 10(a). As can be seen, the pre-compaction pressure of 50MPa results in 10% increase in compression strength while the pre-compaction pressure of 100MPa reduces the compression strength by 31%. Variation of ultimate compression strength of the nanocomposite samples versus volume fraction of reinforcing particles for different pre-compaction pressures are depicted in Fig. 10(b). As it is seen, regardless of the volume percentages of SiC particles, by increasing the pre-compaction pressure from 0 to 50MPa the ultimate strength improves in average by10%. This is while by increasing the pre-compaction pressure from 50 to 100MPa the ultimate

strength reduces by around 31%.

Fig. 11(a) shows the stress–strain curves of Mg-5vol.%SiC fabricated by DH at different pre-compaction stresses. As can be observed, the pre-compaction pressure of 50MPa results in around 7% improvement in compression strength while increasing the pre-compaction pressure to 100MPa leads to around 17% decrease in compression strength.

Finally, variation of ultimate compression strength for nanocomposite samples fabricated by DH versus volume percentages of SiC particles for different pre-compaction pressures is presented in Fig. 11(b). As the figure suggests, by increasing the pre-compaction pressure from 50 to 100MPa ultimate strength reduces by around 17%. The reasons for this reduction are the same as those explained in sections 4.1 and 4.2.
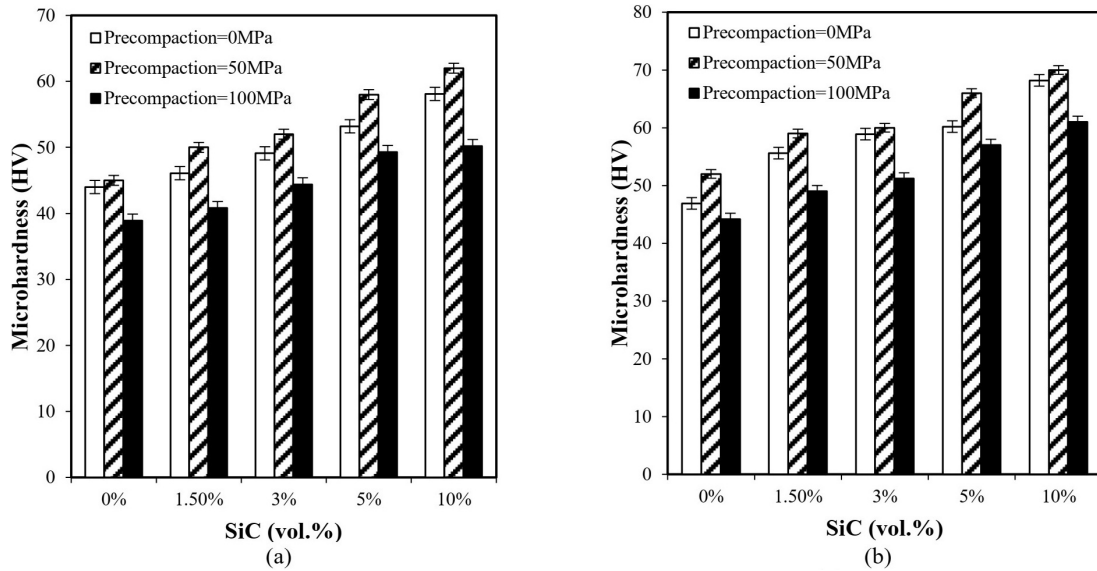

Fig. 9. The effect of pre-compaction on microhardness of nanocomposites fabricated by; a) DH, b) SHB.
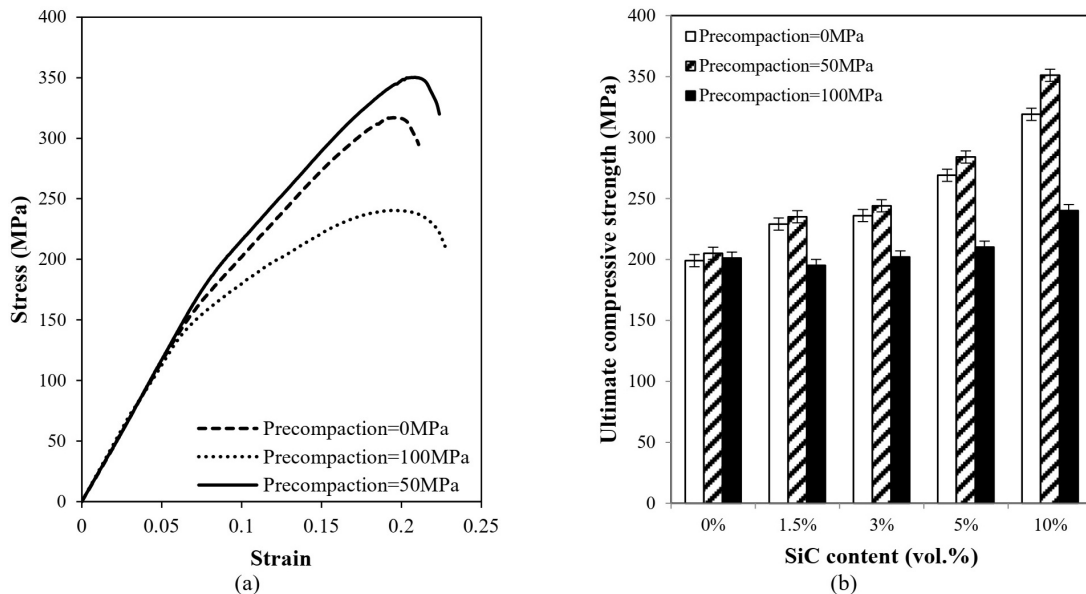

Fig. 10. The effect of pre-compaction on ultimate compressive strength of nanocomposites fabricated by SHB.
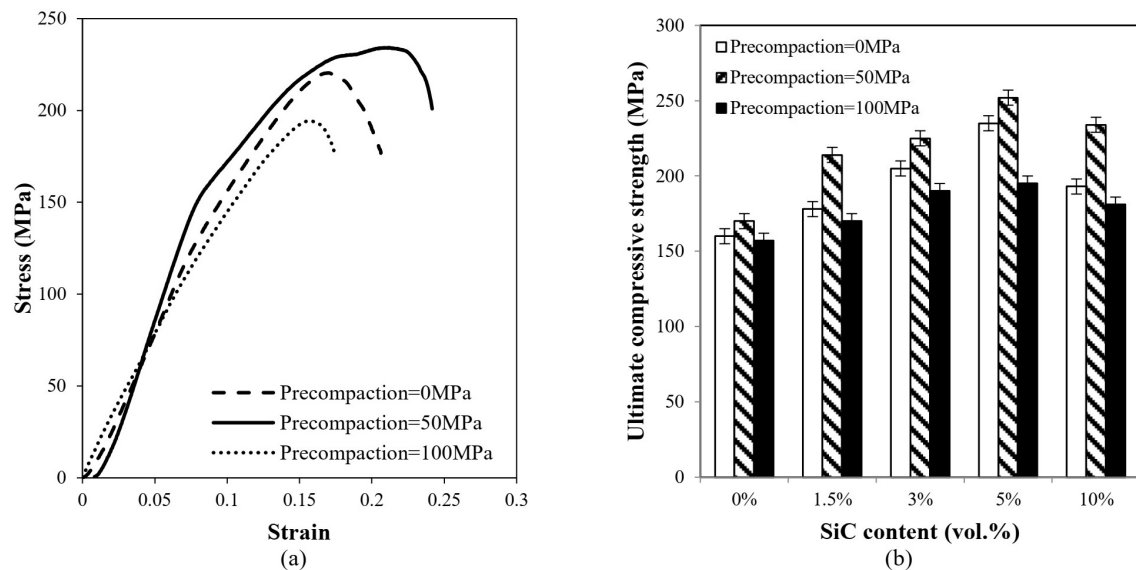
Fig. 11. The effect of pre-compaction on relative density of nanocomposites fabricated by DH.

5. Conclusions

It seems that there is an optimum for the pre-compaction pressure. This optimum varies depending on the type of matrix, reinforcing particles, and compaction loading rate and must be determined for each different case. However, for the nanocomposite studied in this work, Mg/SiC, the following conclusions may be derived:

1. Microstructural examinations revealed that the pre-compaction pressure of 50MPa caused less pores compared to the 100MPa pre-compaction pressure.

2. The pre-compaction pressure of 50MPa improved the relative density of the samples produced under dynamic loading by around 0.7% while for the pressure of 100MPa, relative density reduced by nearly 1.8%.

3. The hardness of the samples pre-compacted at the pressure of 50MPa, increased by 6.7% while the microhardness of the samples pre-compacted at 100MPa decreased by 13%.

4. The pre-compaction pressure of 50MPa resulted in 7 and 10% increase in ultimate strength of samples fabricated using DH and SHB, respectively. The ultimate strength of the samples produced using the pressure of 100MPa reduced by around 17 and 24%, for the samples produced by DH and SHPB, respectively.

References

[1] E.D. Francis, N.E. Prasad, C. Ratnam, P.S. Kumar, V.V. Kumar, Synthesis of nano alumina reinforced magnesium-alloy composites, Int. J. Adv. Sci. Technol., 27 (2011) 35-44.

[2] K. Rahmani, G.H. Majzoobi, An investigation on SiC volume fraction and temperature on static and dynamic behavior of Mg-SiC nanocomposite fabricated by powder metallurgy, Modares Mechanical Engineering, 18 (2018) 361-368.

[3] A. Ahmed, A.J. Neely, K. Shankar, P. Nolan, S. Moricca, T. Eddowes, Synthesis, Tensile Testing, and Microstructural Characterization of Nanometric SiC Particulate-Reinforced Al 7075 Matrix Composites, Metall. Mater. Trans. A, 41(6) (2010) 1582-1591.

[4] J. Onoro, M.D. Salvador, L.E.G. Cambronero, High-temperature mechanical properties of aluminium alloys reinforced with boron carbide particles, Mater. Sci. Eng. A, 499(1-2) (2009) 421-426.

[5] R.M. Mohanty, K. Balasubramanian, S.K. Seshadri, Boron carbide-reinforced alumnium 1100 matrix composites: fabrication and properties, Mater. Sci. Eng. A, 498(1-2) (2008) 42-52.

[6] D.A. Fredenburg, N.N. Thadhani, T.J. Vogler, Shock consolidation of nanocrystalline 6061-T6 aluminum powders, Mater. Sci. Eng. A, 527(15) (2010) 3349-3357.

[7] M.A. Meyers, D.J. Benson, E.A. Olevsky, Shock consolidation: microstructurally-based analysis and computational modeling, Acta Mater., 47(7) (1999) 2089-2108.

[8] K. Rahmani, G.H. Majzoobi, A. Atrian, Simultaneous effects of strain rate and temperature on mechanical response of fabricated Mg–SiC

nanocomposite, J. Compos. Mater., (2019) DOI: 0021998319864629.

[9] G.H. Majzoobi, K. Rahmani, A. Atrian, Temperature effect on mechanical and tribological characterization of Mg-SiC nanocomposite fabricated by high rate compaction, Mater. Res. Express, 5(1) (2018) 015046.

[10] J. Wang, H. Yin, X. QU, Analysis of density and mechanical properties of high velocity compacted iron powder, Acta Metall. Sinica, 22 (2009) 447-453.

[11] W.H. Gourdin, Dynamic consolidation of metal powders, Prog. Mater Sci., 30(1) (1986) 39-80.

[12] ASM International. ASM handbook: Volume 7: Powder Metal Technologies and Applications, Materials Park, OH: ASM International, (1998).

[13] B. Azhdar, B. Stenberg, L. Kari, Development of a high-velocity compaction process for polymer powders, Polym. Test., 24(7) (2005) 909-919.

[14] C.E. Ruegger, M. Çelik, The influence of varying precompaction and main compaction profile parameters on the mechanical strength of compacts, Pharm. Dev. Technol., 5(4) (2000) 495-505.

[15] E.P. Carton, M. Stuivinga, H.J. Verbeek, Crack prevention in shock compaction of powders, AIP Conference Proceedings, 429(1) (1998) 549-552.

[16] M. Stuivinga, E.P. Carton, J.R. de Wijn, Shock compaction of bioceramic composites, in: EXPLOMET 2000, International Conference on Fundamental Issues and Applications of Shock-Wave and High-Strain-Rate Phenomena, Albuquerque, New Mexico, USA, (2000) 19-22.

[17] G.H. Majzoobi, A. Atrian, M. Pipelzadeh, Effect of densification rate on consolidation and properties of Al7075–B_4C composite powder, Powder Metall., 58 (2015) 281-288.

[18] A. Atrian, G.H. Majzoobi, H. Bakhtiari, The effect of pre-compaction on dynamic compaction process of Al/SiC nanocomposite powder, The Bi-Annual International Conference on Experimental Solid Mechanics and Dynamics (X-Mech-2014), (2014).

[19] S.J. Hong, J.M. Koo, J.G. Lee, M.K. Lee, H.H. Kim, C.K. Rhee, Precompaction Effects on Density and Mechanical Properties of Al_2O_3 Nanopowder Compacts Fabricated by Magnetic Pulsed Compaction, Mater. Trans., 50 (2009) 2885-2890.

[20] M.J. Yi, H.Q. Yin, J.Z. Wang, X.J. Yuan, X.H. Qu, Comparative research on high-velocity compaction and conventional rigid die compaction, Front. Mater. Sci. China, 3(4) (2009) 447.

[21] K. Rahmani, G.H. Majzoobi, A. Atrian, A novel approach for dynamic compaction of Mg–SiC nanocomposite powder using a modified Split Hopkinson Pressure Bar, Powder Metall., 61(2) (2018) 164-177.

[22] G.H. Majzoobi, H. Bakhtiari, A. Atrian, M.K. Pipelzadeh, S. Hardy, Warm dynamic compaction of Al6061/SiC nanocomposite powders, Proc. Inst. Mech. Eng. L, 230(2) (2016) 375-387.

[23] A. Nayeem Faruqui, P. Manikandan, T. Sato, Y. Mitsuno, K. Hokamoto, Mechanical milling and synthesis of Mg-SiC composites using underwater shock consolidation, Met. Mater. Int., 18(1) (2012) 157-163.

[24] ASTM, Standard Practice for Microetching Metals and Alloys, in, United Stated of America: ASTM, (2005).

[25] ASTM E384-00 Test Method for Microindentation Hardness of Materials, American Society for Testing and Materials International, Volume 03.01, W. Conshohocken, PA, (2003).

[26] Standard, Standard test methods of compression testing of metallic materials at room temperature, 1990 Annual Book of ASTM Standards, ASTM, West Conshohocken, PA, (1990) 98-105.

[27] G.H. Majzoobi, K. Rahmani, A. Atrian, An experimental investigation into wear resistance of Mg-SiC nanocomposite produced at high rate of compaction, J. Stress Anal., 3(1) (2018) 35-45.